cations (*10*–*12*) or for fabrication of integrated magnetic memory devices or sensors (*25*). It could also be of interest for ultrahigh density near-field optical recording (*26*, *27*), because optical properties also may be locally changed by adjusting the irradiation conditions.

REFERENCES AND NOTES

1. E. Grochowski and D. A. Thompson, *IEEE Trans. Magn.* **MAG-30**, 3797 (1994).
2. D. N. Lambeth, E. M. T. Velu, G. H. Bellesis, L. L. Lee, D. E. Laughlin, *J. Appl. Phys.* **79**, 4496 (1996).
3. S. Gadetsky, J. K. Erwin, M. Mansuripur, *ibid*., p. 5687 (1996).
4. S. Y. Chou, M. S. Wei, P. R. Krauss, P. Fischer, *ibid.* **76**, 6673 (1994).
5. S. Y. Chou, P. R. Krauss, P. J. Renstrom, *Science* **272**, 85 (1996).
6. Y. Xia, X. M. Zhao, G. M. Whitesides, *Microelecton. Eng.* **32**, 255 (1996).
7. Y. Chen *et al*., *J. Vac. Sci. Technol. B* **12**, 3959 (1994).
8. A. Fernandez, P. J. Bedrossian, S. L. Baker, S. P. Vernon, D. R. Kania, *IEEE Trans. Magn. Mag.* **32**, 4472 (1996).
9. J. L. Simonds, *Phys. Today* **48** (no. 4), 26 (1995).
10. E. Betzig *et al*., *Appl. Phys. Lett.* **61**, 142 (1992).
11. B. D. Terris, H. J. Mamin, D. Rugar, W. R. Studenmund, G. S. Kino, *ibid.* **65**, 388 (1994).
12. T. J. Silva, S. Schultz, D. Weller, *ibid.*, p. 658.
13. M. Mansuripur, *The Physical Principles of Magneto-Optical Recording* (Cambridge Univ. Press, Cambridge, 1995).
14. V. Kottler, N. Essaidi, N. Ronarch, C. Chappert, Y. Chen, *J. Magn. Magn. Mater.* **165**, 398 (1997); V. Kottler, C. Chappert, N. Essaidi, Y. Chen, *IEEE Trans. Magn.*, in press.
15. M. G. Le Boité, A. Traverse, L. Névot, B. Pardo, J. Corno, *J. Mater. Res.* **3**, 1089 (1988); M. G. Le Boité, A. Traverse, H. Bernas, C. Janot, J. Chevrier, *Mater. Lett.* **6**, 173 (1988); A. Traverse, M. G. Le Boité, G. Martin, *Europhys. Lett.* **8**, 633 (1989).
16. After a soft radio frequency (rf) etch of the substrate, a 6.5-nm-thick Pt buffer layer is first deposited at about 0.25 nm/s using dc magnetron (at an Ar pressure of 5×10^{-3} mbar), which gives a flat continuous polycrystalline film with nearly perfect (111) texture and small (~7 nm) grain size. Then rf diode and rf magnetron, respectively, are used for deposition of the Co and Pt layers at around 0.02 nm/s, terminating all samples with a 3.4-nm Pt coverage layer. AFM measurements show a root mean square roughness of the Pt buffer layer around 0.2 nm, which is preserved on the topmost surface (Pt coverage layer) for all samples.
17. S. Lemerle *et al*., in *Magnetic Hysteresis in Novel Magnetic Materials*, *NATO ASI Series E: Applied Sciences–338*, G. C. Hadjipanayis, Ed. (Kluwer Academic, Dordrecht, Netherlands, 1997), pp. 537–542.
18. L. Belliard *et al*., *J. Appl. Phys.* **81**, 5315 (1997).
19. J. P. Deville, A. Barbier, C. Boeglin, B. Carrière, *Mater. Res. Soc. Symp. Proc.* **313**, 519 (1993).
20. J. Pommier *et al., Phys. Rev. Lett.* **65**, 2054 (1990).
21. J. Ziegler, J. Biersack, U. Littmark, *The Stopping and Range of Ions in Solids* (Pergamon, New York, 1985).
22. T. Massalski, *Binary Alloy Phase Diagrams* (Metals Information Society, Metals Park, OH, ed. 2, 1990).
23. We have not yet studied these limits experimentally but have performed simulations (T. Devolder *et al*., unpublished data) to determine the length (hereafter called "transition length") over which ion-induced structural changes occur at a mask edge. The limiting factor of the transition length is not the ion beam angular spread but the ion beam lateral straggling values at the Pt-Co layer depth, which in turn depend on the mask thickness seen by the ion beam in case of incomplete stopping. To determine the effect of a lithographically made irradiation mask on the transition length, we performed calculations for a PMMA stripe (200 nm wide, 600 nm high, with both a vertical- and a pyramid-based edge profile deduced from scanning electron micrographs of real masks). Transition length estimates were obtained by convoluting mask shapes corresponding to our experimental conditions with lateral straggling values deduced from TRIM simulations (*19*). Depending on the exact shapes assumed for the former, the obtainable lateral resolution for PMMA masks varied from 100 nm (worst case) to 20 nm (best case). We anticipate that even lower values (down to about 5 nm or less) might be obtained by using more appropriate masks and patterning techniques; see, for example, [R. M. H. New, R. F. W. Pease, R. L. White, *J. Vac. Sci. Technol.* B **12**, 3196 (1994)]. The fact that the magnetic property changes are not related in a simple way to the ion-induced structural changes must be considered. In separate studies (unpublished data) of unmasked Co-Pt structures, we determined the ion fluence dependence of the Kerr rotation and the anisotropy, from which we can estimate the transition length for magnetic property changes. We find that in most cases the magnetic transition will be sharper than the structural one.
24. M. Cai *et al*., *J. Appl. Phys.* **81**, 5200 (1997).
25. M. Johnson *et al*., *Appl. Phys. Lett.* **71**, 974 (1997).
26. B. D. Terris, H. J. Mamin, D. Rugar, *ibid.* **68**, 141 (1996).
27. Y. Martin, S. Rishton, H. K. Wickramasinghe, *ibid.* **71**, 1 (1997).

28. We thank O. Kaitasov and S. Gautrot for technical assistance. This work was performed within the framework of the ISARD collaboration (Université Paris–Sud). V. K. is funded by a Marie-Curie grant from the European Union.

1 December 1997; accepted 29 April 1998

Post-Cambrian Trilobite Diversity and Evolutionary Faunas

Jonathan M. Adrain,* Richard A. Fortey, Stephen R. Westrop

A cluster analysis of the stratigraphic distribution of all Ordovician trilobite families, based on a comprehensive taxonomic database, identified two major faunas with disjunct temporal diversity trends. The Ibex Fauna behaved as a cohort, declining through the Ordovician and disappearing at the end-Ordovician mass extinction. In contrast, the Whiterock Fauna radiated rapidly during the Middle Ordovician and gave rise to all post-Ordovician trilobite diversity. Its pattern of diversification matches that of the Paleozoic Evolutionary Fauna; hence, trilobites were active participants in the great Ordovician radiations. Extinction patterns at the end of the Ordovician are related to clade size: Surviving trilobite families show higher genus diversity than extinguished families.

Trilobites are among the most common fossils of the Early Paleozoic, and an understanding of their history is central to any hypothesis of the development of the marine biosphere during this time. Cumulative trilobite diversity (*1*) is often portrayed as a bottom-heavy spindle diagram derived by counting genera or families recognized during particular epochs. The most current description of cumulative taxonomic diversity is Sepkoski's compendium of marine families (*2*) and genera (*3*) and his seminal factor-analytical description of the marine record (*4*). We used a new comprehensive genus-level global data set to reinvestigate patterns of post-Cambrian trilobite diversity.

Trilobite diversity has been understood in relation to three major events in the Early Phanerozoic history of life: the Cambrian explosion (*5*), the Ordovician radiation (*6*), and the end-Ordovician mass extinction (*7*). Of these events, the diversity pattern of trilobites after the Cambrian explosion is uncontroversial; with the advent of mineralized hard parts, trilobites radiated rapidly and soon reached their peak clade diversity (*8*). The role of trilobites in the Ordovician events is less well understood. The class was in modest decline during the time of the Ordovician radiation (*1*, *3*, *4*), along with other elements of the Cambrian Evolutionary Fauna (*4*). Trilobites were one of the groups most affected by the end-Ordovician extinction, and most estimates record a loss of about half of familial or generic diversity at this event (*3*, *4*). Post-Cambrian trilobite history has therefore been inferred to follow a general and sustained decline, or a decay of a high-diversity Early Ordovician cohort (*9*). However, the cumulative diversity curve poorly reflects some important features of trilobite history: (i) No natural subgroup of trilobites (monophyletic order, superfamily, or family) has an Ordovician-Silurian diversity history matching the shape of the cumulative plot. Although components may have different diversity histories from cumulative trends, no clade among the trilobites is even similar to the curve for the Ibex (Lower Ordovician) through Wenlock (Silurian) series.

J. M. Adrain and R. A. Fortey, Department of Palaeontology, Natural History Museum, Cromwell Road, London SW7 5BD, UK.
S. R. Westrop, Oklahoma Museum of Natural History and School of Geology and Geophysics, University of Oklahoma, Norman, OK 73019, USA.

*To whom correspondence should be addressed. E-mail: j.adrain@nhm.ac.uk

(ii) There are few examples of surviving Silurian trilobite families that record sustained diversity reductions across the Ordovician-Silurian boundary, even though cumulative trilobite diversity was reduced by nearly half. (iii) Many trilobite groups show increases in diversity during the time of the Ordovician radiations, even though cumulative trilobite diversity was in decline. These observations suggest that the cumulative trilobite diversity curve is an amalgam of more than one major pattern.

Our survey recognizes 1241 validly proposed Ordovician and Lower Silurian trilobite genera. We carried out comprehensive taxonomic standardization (*10*) resulting in the recognition of 296 subjective junior synonyms, leaving 945 accepted genera (*11*). The occurrence of each genus was plotted by stratigraphic series (*12*). Genera were then assigned to monophyletic families, and the families were used as the principal units for further analysis. Cluster analysis (*13*) grouped families according to their numbers of component genera in each of the four Ordovician stratigraphic series (Ibex, Whiterock, Mohawk and Cincinnati). To test the behavior of families at the end-Ordovician events, we omitted Silurian occurrences in the cluster analysis.

Together, dendrograms and histograms showing diversity histories of all families (Fig. 1) indicate that the trilobites form two major clusters (*14*), termed faunas. The Ibex Fauna, named for the epoch during which it flourished, is characterized by Early Ordovician dominance followed by severe diversity reductions in the later Ordovician (conforming to a null hypothesis of cohort decay). The Whiterock Fauna, named for the epoch in which it radiated rapidly, displays a contrasting pattern of minimal Early Ordovician diversity, Middle Ordovician (Whiterock) radiation, and high Late Ordovician diversity. These alternate, disjunct patterns are pervasive and represent high-level macroevolutionary trends. Surviving Silurian families constitute a subgroup of the Whiterock Fauna, termed the Silurian Fauna (*15*).

The base of the North American Whiterock Series (*16*) has been recognized as marking the start of the great Ordovician radiations of articulate brachiopods (*17*), bryozoans (*18*), bivalves (*19*), echinoderms (*20*), and virgellinid graptoloids (*21*); many other groups first occur in the rock record at or near this horizon (*3*, *6*, *22*). This also marks the point of transition between dominance of Sepkoski's (*4*, *23*) Cambrian Evolutionary Fauna (of which trilobites are the main component) and the rise of the Paleozoic Evolutionary Fauna (composed of the radiating groups). The Whiterock Fauna shows explosive and sustained radiation at exactly this point, conforming to the Paleozoic fauna diversity pattern; this indicates that trilobites were active participants in the Ordovician radiation. Most individual trilobite genera in the study interval (503, or 53.2% of the total) belong to families

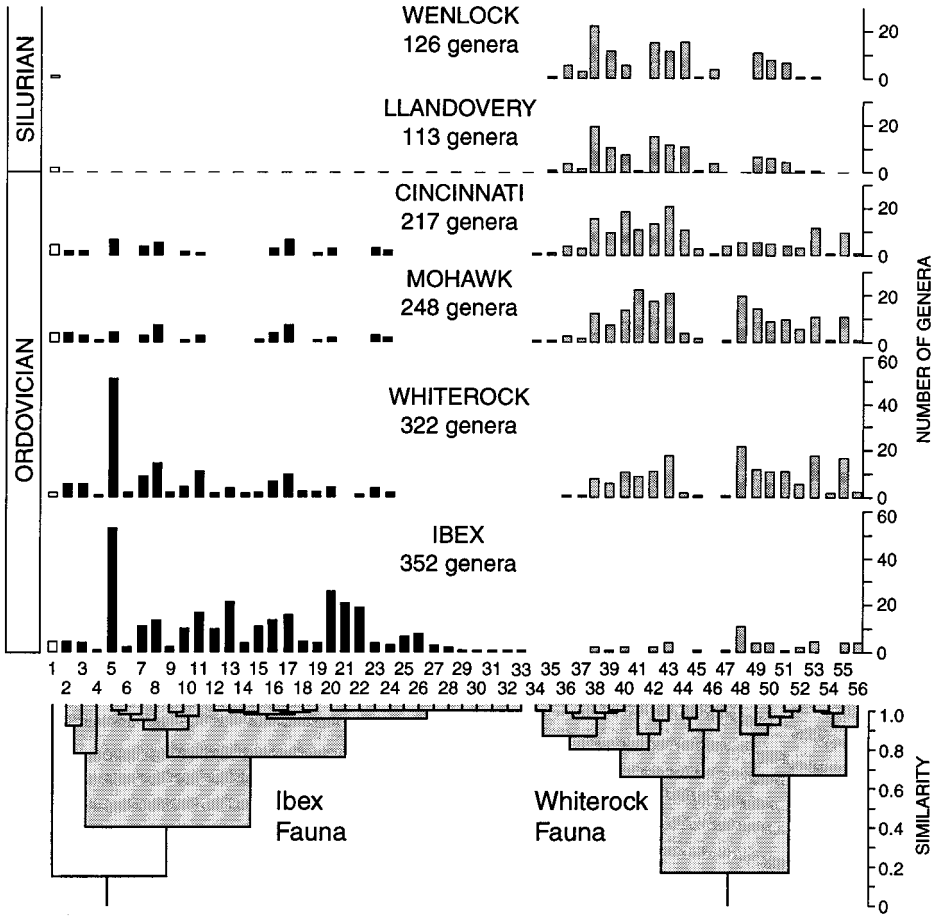

Fig. 1. Cluster analysis of all Ordovician and Lower Silurian trilobite families, with plots of their diversity through time. Clustering was based on Ordovician diversities only. Taxa were clustered using as variables the number of genera in each of the four Ordovician biostratigraphic intervals. The Pearson product-moment correlation coefficient was used as the index of similarity; the clusters were formed using the average linkage method. Families are numbered as follows: 1, Harpetidae; 2, Dimeropygidae; 3, Telephinidae; 4, Prosopiscidae; 5, Asaphidae; 6, Raymondinidae; 7, Nileidae; 8, Pliomeridae; 9, Bathycheilidae; 10, Shumardiidae; 11, Bathyuridae; 12, Hungaiidae; 13, Leiostegiidae; 14, Entomaspididae; 15, Alsataspididae; 16, Agnostidae; 17, Remopleurididae; 18, Taihungshaniidae; 19, Panderiidae; 20, Olenidae; 21, Hystricuridae; 22, Pilekiidae; 23, Isocolidae; 24, Pharostomatidae; 25, Eulomidae; 26, Ceratopygidae; 27, Lichakephalidae; 28, Bavarillidae; 29, Dikelocephalidae; 30, Idahoiidae; 31, Nepeidae; 32, Norwoodiidae; 33, Solenopleuridae; 34, Ityophoridae; 35, Brachymetopidae; 36, Aulacopleuridae; 37, Acastidae; 38, Odontopleuridae; 39, Lichidae; 40, Illaenidae; 41, Pterygometopidae; 42, Encrinuridae; 43, Cheiruridae; 44, Proetidae; 45, Scharyiidae; 46, Phacopidae; 47, Rorringtoniidae; 48, Trinucleidae; 49, Styginidae; 50, Calymenidae; 51, Dalmanitidae; 52, Homalonotidae; 53, Raphiophoridae; 54, Bohemillidae; 55, Cyclopygidae; and 56, Dionididae.

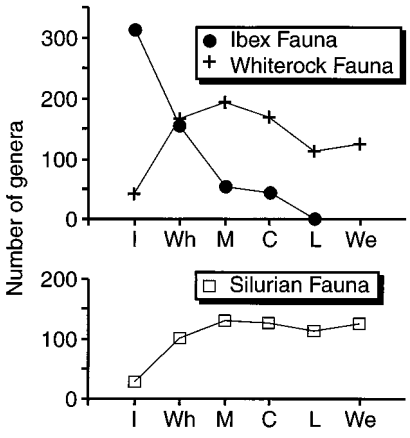

Fig. 2. Line graphs of the total diversity of each major fauna in each of the six biostratigraphic intervals (I, Ibex; Wh, Whiterock; M, Mohawk; C, Cincinnati; L, Llandovery; and We, Wenlock). Ibex and Whiterock faunas are as defined in Fig. 1. The Silurian Fauna is a subset of the Whiterock Fauna comprising those groups that survived the end-Ordovician extinction, minus two single-lineage relicts (*15*).

comprising the Whiterock Fauna.

The Ordovician diversity patterns also predict the fate of clades at the end-Ordovician mass extinctions (Fig. 2). No member of the Ibex Fauna survived the end of the Ordovician. In contrast, nearly three-fourths of families (74%) of the Whiterock Fauna survived, and the Whiterock Fauna accounts for all post-Ordovician trilobites, with the exception of the unclustered harpetids.

Because the Ibex Fauna was showing a general decline in diversity before the end of the Ordovician while the Whiterock Fauna was undergoing robust radiation, we infer that clade survival at the end-Ordovician extinction was related to clade size. Comparison of frequency distributions of clade sizes for 37 families present in the latest Ordovician Cincinnati Series (Fig. 3) demonstrates that survivors have larger genus diversity (mean, 8.3 genera) than those families that were extinguished (mean, 3.6 genera). The influence of clade size on survival contrasts with patterns of molluscan genus survival at the end-Cretaceous event (*24*), gastropod genus survival at the end-Permian event (*25*), and trilobite family survival at the end of the Cambrian (*26*), all of which were unrelated to clade size.

These patterns are influenced by genus origination rates (Fig. 4). The decay of the Ibex Fauna cohort was driven by low post-Whiterock origination. The genus originations of the Whiterock Fauna were at times more than double those of the Ibex Fauna. This high rate led to larger mean clade sizes, effectively buffering Whiterock Fauna families from end-Ordovician extinction.

Silurian Fauna groups show only a small diversity reduction at the series level (10 genera, or 8.4% of Cincinnati diversity) from Upper Ordovician to earliest Silurian. From a high in the Mohawk level of 127 genera to the Wenlock level of 124 genera, there is series-level variation of only 14% of the maximum. Although the long-term diversity of most surviving trilobite groups was essentially unchanged, the end-Ordovician extinction had a significant short-term impact on the Silurian Fauna. Of the Silurian Fauna genera present during the Llandovery epoch, 78% also originated in that epoch (Fig. 4), which demonstrates that extinctions were followed by a rapid post-extinction "rebound" (*3, 4*). However, once this Llandovery rebound was completed, standing diversity returned to and was maintained at pre-extinction amounts.

End-Ordovician fates are linked to Ordovician diversity trajectories. Most extinguished groups were members of the Ibex Fauna and had already undergone sustained and severe diversity culls after the Early Ordovician. The absolute decline in diversity involved in the end-Ordovician disappearance of the Ibex Fauna was about half the magnitude of its Whiterock-Mohawk drop (67% reduction) and about one-third the magnitude of the Ibex-Whiterock drop (48% reduction) (Fig. 2). Physical environmental changes were linked to the end-Ordovician extinction of some trilobite clades (*7*); the relatively sudden decimation of Whiterock Fauna families such as Cyclopygidae and Raphiophoridae is otherwise difficult to explain (*27*). Nevertheless, the diversity model we propose casts new light on the nature of the end-Ordovician trilobite decline. Most of the clades that became extinct were already in long-term decline, whereas most of the clades that survived suffered no sustained diversity reduction after the extinction.

The pattern of diversification of the Whiterock Fauna has several implications for the Ordovician radiation. This event was one of the largest diversity increases in the history of life, comparable in magnitude only to the Cambrian evolutionary explosion. It involved a complete reorganization of benthic marine communities, as trilobite-dominated assemblages of the Cambrian and Early Ordovician were replaced by brachiopod-rich associations characteristic of Sepkoski's (*3, 4*) Paleozoic Fauna. One of the central themes of investigation of the Ordovician radiation has been the hypothesis (*28*) of onshore development of the Paleozoic Fauna and concomitant offshore displacement and restriction of the Cambrian Fauna (of which trilobites are the main constituent) through time. It has been demonstrated (*29*) that the diminished ecologic importance of trilobites as a whole in onshore environments most likely resulted from dilution rather than physical displacement. Alpha (within-community) diversity of trilobites is stable in all environments throughout the Ordovician. This contrasts markedly with the major fluctuations in clade patterns presented here, and suggests an unexpected decoupling of global taxonomic diversity and local ecological success through the Middle and Upper Ordovician (*30*).

There is a strong zoogeographic component to the radiation of the Whiterock Fauna. Of the 21 families present during the early Whiterock, eight had a predominantly low-latitude distribution on the Laurentian paleocontinent (*31*), nine were restricted to high-latitude Gondwanaland and Baltica, and four were cosmopolitan. However, histograms of clade sizes (Fig. 1) indicate that the radiation of the Whiterock Fauna was more pronounced at low latitudes (Laurentian groups experienced a genus increase of more than 500%, versus about 300% for Gondwanan and Baltic families). Furthermore, end-Ordovician survival was markedly higher among Whiterock Fauna groups that initially diversified at low versus high latitudes. All eight Laurentian families survived the end-Ordovician extinction, compared with only three of the nine Gondwanan/Baltic groups. Groups that had a Laurentian early distribution account for the bulk of the Silurian Fauna.

This latitudinal contrast between radiation intensity and survivorship also extends to the ecological context of the radiation. Whiterock Fauna groups that diversified in the clastic environments of Gondwanaland occur in a broad bathymetric and environmental range, a distribution difficult to distinguish from that of coeval elements of the Ibex Fauna. However, the tropical Laurentian origins of the Silurian Fauna (*32*) were almost exclusively in platform-margin environments. Shallow-water Laurentian faunas (*33*) were dominated by the Ibex Fauna at the onset of the radiation, although the Whiterock Fauna rapidly spread onshore. This pattern is of considerable importance and requires further study because it implies

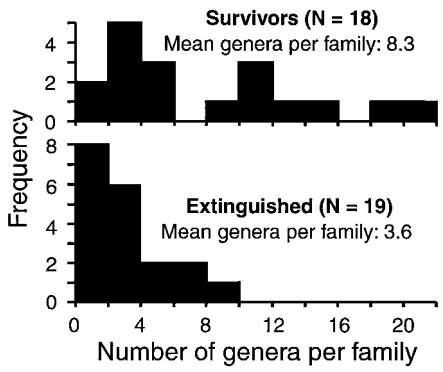

Fig. 3. Frequency distribution of clade size, measured by number of genera, for trilobite families present in the Upper Ordovician (Cincinnati) that survived (upper panel) or became extinct (lower panel) at the end-Ordovician. The distributions are significantly different (Mann-Whitney *u* test, $P = 0.01$). Surviving families have a mean Cincinnati diversity of 8.3 genera, whereas the value for extinguished families is 3.6 genera.

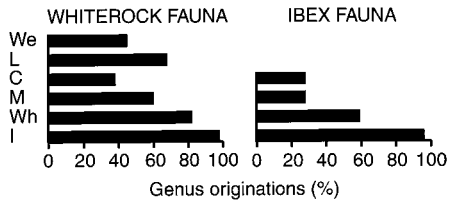

Fig. 4. Genus origination of each major fauna in each of the six biostratigraphic intervals. Originations are shown as the percentage of the total number of genera present in the interval that have their first occurrence in that interval.

that the radiation of the Whiterock trilobite fauna was initiated in more offshore settings than that of the Paleozoic Fauna.

In assessing the reasons for the differing responses of trilobite groups during the Ordovician radiation, it will ultimately be necessary to understand their early phylogenetic history. Many problems remain in resolving trilobite relationships across the Cambro-Ordovician boundary (*34*). However, it is principally Ibex Fauna families that have known or suspected Cambrian distributions. Whiterock Fauna families, and in particular Silurian Fauna groups, can generally be traced only to the Early Ordovician, and in many cases they are entirely "cryptogenetic." These clades certainly had Cambrian forebears, but the fact that they have avoided detection is a strong indication that novel morphologies were being developed very rapidly. This implied difference in rates of evolution is testable through analysis of species turnover, and is perhaps the most compelling clue to the strikingly disjunct fates of post-Cambrian trilobites.

REFERENCES AND NOTES

1. A. T. Thomas and R. A. Fortey, in *Atlas of Invertebrate Macrofossils,* J. W. Murray, Ed. (Longman, London, 1985), pp. 199–229; R. A. Robison, in *Fossil Invertebrates*, R. S. Boardman, A. H. Cheetham, A. J. Rowell, Eds. (Blackwell, Palo Alto, CA, 1987), pp. 221–241.
2. J. J. Sepkoski Jr., *Milwaukee Public Mus. Contrib. Biol. Geol.* **83**, 1 (1992).
3. The full data set has not yet been published, but preliminary plots are given by J. J. Sepkoski Jr., in (*22*), pp. 393–396.
4. _____, *Paleobiology* **7**, 36 (1981).
5. R. A. Fortey, D. E. G. Briggs, M. A. Wills, *Bioessays* **19**, 429 (1997).
6. M. L. Droser, R. A. Fortey, X. Li, *Am. Sci.* **84**, 122 (1996).
7. P. J. Brenchley, in *Mass Extinctions: Processes and Evidence*, S. K. Donovan, Ed. (Belhaven, London, 1990), pp. 104–132.
8. R. A. Fortey and R. M. Owens, in *Major Evolutionary Radiations*, P. D. Taylor and G. P. Larwood, Eds. (Systematics Association Special Volume 42, Clarendon, Oxford, 1990), pp. 139–164.
9. M. Foote, *Paleobiology* **14**, 258 (1988).
10. S. J. Culver, M. A. Buzas, L. S. Collins, *ibid*. **13**, 169 (1987).
11. The full database will be published elsewhere; a current version is available from the senior author on request.
12. We used North American Ordovician series, but the globally correlative *Nemograptus gracilis* Zone is included in the Mohawk, instead of its traditional assignment to the upper Whiterock. This revision is based on the recent recommendations of the Subcommission on Ordovician Stratigraphy and results in more satisfactory sampling intervals. At the series level of resolution, there are few examples of Lazarus taxa (taxa occurring earlier and later than, but not within, a given sampling interval); where such sampling gaps occurred, genera were scored as present.
13. Principal components analysis of the data set confirmed the division into two major faunas. The groupings are so robust that the use of alternative similarity indices will not significantly alter the result.
14. A single family, Harpetidae, falls outside the two major clusters. The generic taxonomy of this group is in need of revision.
15. We define the Silurian Fauna as Whiterock Fauna families in which at least one lineage survived the end-Ordovician extinction and subsequently diversified, thus excluding two minor relict distributions, Pterygometopidae and Raphiophoridae, in each of which a single low-diversity lineage extended into the Silurian but became extinct during the period.
16. Upper Arenig in British terminology.
17. M. E. Patzkowsky, in (*22*), pp. 413–414.
18. R. L. Anstey and J. F. Pachut, in *New Approaches to Speciation in the Fossil Record*, D. H. Erwin and R. L. Anstey, Eds. (Columbia Univ. Press, New York, 1995), pp. 239–284.
19. J. C. W. Cope, *Palaeontology* **39**, 979 (1996); *ibid.* **40**, 713 (1997); J. Pojeta and J. Gilbert-Tomlinson, *Bull. Bur. Miner. Res. Geol. Geophys.* **174**, 1 (1977).
20. J. Sprinkle, in *Origins and Early Evolution of the Metazoa*, J. H. Lipps and P. W. Signor, Eds. (Plenum, New York, 1992), pp. 375–398.
21. R. A. Fortey and R. A. Cooper, *Palaeontology* **29**, 631 (1986).
22. M. L. Droser, P. M. Sheehan, R. A. Fortey, X. Li, in *Ordovician Odyssey: Short Papers for the Seventh International Symposium on the Ordovician System*, J. D. Cooper, M. L. Droser, S. C. Finney, Eds. (Pacific Section Society for Sedimentary Geology, Fullerton, CA, 1995), pp. 405–408.
23. J. J. Sepkoski Jr., in *Short Papers for the Second International Symposium on the Cambrian System*, M. E. Taylor, Ed. (USGS Open-File Rep. 81-743, 1981), pp. 203–207.
24. D. Jablonski, *Science* **231**, 129 (1986).
25. D. H. Erwin, *Paleobiology* **16**, 187 (1990).
26. S. R. Westrop, *ibid*. **15**, 46 (1989).
27. Physical causes of end-Ordovician trilobite extinction were proposed by R. A. Fortey, *Philos. Trans. R. Soc. London Ser. B* **325**, 327 (1989); B. D. E. Chatterton and S. E. Speyer, *Paleobiology* **15**, 118 (1989).
28. J. J. Sepkoski Jr. and A. I. Miller, in *Phanerozoic Diversity Patterns: Profiles in Macroevolution*, J. W. Valentine, Ed. (Princeton Univ. Press, Princeton, 1985), pp. 153–190; J. J. Sepkoski Jr. and P. M. Sheehan, in *Biotic Interactions in Recent and Fossil Benthic Communities*, M. J. S. Tevesz and P. M. McCall, Eds. (Plenum, New York, 1983), pp. 673–717.
29. S. R. Westrop, J. V. Tremblay, E. Landing, *Palaios* **10**, 75 (1995); S. R. Westrop and J. M. Adrain, *Paleobiology* **24**, 1 (1998).
30. Work in progress suggests that this disassociation of clade and alpha diversity continued well into the Silurian [J. M. Adrain, *Geol. Soc. Am. Abstr. Programs* **28**, A291 (1996)].
31. For paleogeographic reconstructions, see W. S. McKerrow and C. R. Scotese, Eds., *Palaeozoic Palaeogeography and Biogeography*, *Geol. Soc. London Mem. 12* (1990).
32. H. B. Whittington, *Bull. Mus. Comp. Zool. Harv. Univ.* **129**, 1 (1963); J. M. Adrain and R. A. Fortey, *Bull. Nat. Hist. Mus. London Geol. Ser.* **53**, 79 (1997).
33. R. A. Fortey and M. L. Droser, *J. Paleontol.* **70**, 73 (1996).
34. H. B. Whittington, *Geol. Mag.* **118**, 591 (1981); R. A. Fortey, *Spec. Pap. Palaeontol.* **30**, 179 (1983); G. D. Edgecombe, in *Extinction and Phylogeny*, M. J. Novacek and Q. D. Wheeler, Eds. (Columbia Univ. Press, New York, 1992), pp. 144–177.

35. We thank G. D. Edgecombe, J. J. Sepkoski Jr., and A. B. Smith for comments on the manuscript. Preparation of this study was funded by Natural Environment Research Council (UK) grant GR3/09654 and by Natural Sciences and Engineering Research Council (Canada) grant 41197.

19 February 1998; accepted 21 April 1998

Visualization of the Local Insulator-Metal Transition in $Pr_{0.7}Ca_{0.3}MnO_3$

Manfred Fiebig,* Kenjiro Miyano, Yoshinori Tomioka, Yasuhide Tokura

The light-induced insulator-metal transition in the "colossal magnetoresistance" compound $Pr_{0.7}Ca_{0.3}MnO_3$ is shown to generate a well-localized conducting path while the bulk of the sample remains insulating. The path can be visualized through a change of reflectivity that accompanies the phase transition. Its visibility provides a tool for gaining insight into electronic transport in materials with strong magnetic correlations. For example, a conducting path can be generated or removed at an arbitrary position just because of the presence of another path. Such manipulation may be useful in the construction of optical switches.

Manganese oxides of the general formula $R_{1-x}A_xMnO_3$ (where R and A are rare- and alkaline-earth ions, respectively) have recently attracted considerable attention because of their unusual magnetic and electronic properties (*1*). In some of these materials, insulator-metal (I-M) transitions can be observed where both conductivity and magnetization change markedly. The $x = 0$ and $x = 1$ end members of the $R_{1-x}A_xMnO_3$ family are insulating and antiferromagnetic (AF) with the Mn ion in the Mn^{3+} and Mn^{4+} state, respectively. For intermediate x, the average Mn valence is non-integer and the material is generally semiconducting or metallic at high temperatures. Most of the perovskite manganites show a ferromagnetic (FM) ground state when the holes are optimally doped (usually $0.2 \leq x \leq 0.5$) by chemical substitution of the perovskite A-site. However, in com-

M. Fiebig, Department of Applied Physics, The University of Tokyo, Tokyo 113-8656, Japan, and Japan Science and Technology Corporation (JST), Tokyo 171-0031, Japan.
K. Miyano, Department of Applied Physics, The University of Tokyo, Tokyo 113-8656, Japan.
Y. Tomioka, Joint Research Center for Atomic Technology (JRCAT), Tsukuba 305-0046, Japan.
Y. Tokura, Department of Applied Physics, The University of Tokyo, Tokyo 113-8656, Japan, and JRCAT, Tsukuba 305-0046, Japan.

*To whom correspondence should be addressed. E-mail: fiebig@ap.t.u-tokyo.ac.jp